SUPERDOVE-MODELLED BATHYMETRY USING NEURAL NETWORKS ALONG A TURBIDITY GRADIENT: BREHAT, SAINT-BARTHELEMY AND TETIAROA ISLANDS

A. Collin [1] *, P. Palola [2], D. James [1], Y. Pastol [3], C. Monpert [3], S. Loyer [3], B. Stoll [4], E. Feunteun [1], L. Wedding [2]

[1] CGEL, EPHE-PSL University, 35800 Dinard, France – (antoine.collin, dorothee.james, eric.feunteun)@ephe.psl.eu
[2] Oxford Seascape Ecology Lab, University of Oxford, Oxford, OX1 3QY, UK – (pirta.palola, lisa.wedding)@ouce.ox.ac.uk
[3] Shom, 29228 Brest, France – (yves.pastol, coralie.monpert, sophie.loyer)@shom.fr
[4] GePaSud, Université de la Polynésie Française, 98702 Faa'a, Tahiti, French Polynesia – benoit.stoll@upf.pf

KEY WORDS: Bathymetry, Planetscope, High Spatial Resolution, Very High Temporal Resolution, Neural Networks, Lidar.

ABSTRACT:

Despite the increasing interest in the bathymetry mapping in the context of the sea level rise and storm intensification, only 10% of the worldwide bathymetry has been mapped with reliable sonar and lidar, due to their high cost. The satellite-derived bathymetry (SDB) has therefore grown for the last decades, due to its affordability, but also to its gain in radiometric, spatial, spectral and temporal resolutions. Nevertheless, SDB products leveraging both a high spatial and a high temporal resolution are still expected by stakeholders responsible for cloudy or tidal coastal areas. This research tests the contribution of the Planetscope SuperDove CubSats (eight-band, 3 m, 1 day) four novel bands in bathymetry extraction, along a turbidity gradient (the islands of Bréhat in Channel Sea, Saint-Barthélémy in Caribbean Atlantic Ocean, and Teti'aroa in South Pacific Ocean), using neural networks calibrated, validated, and tested with recent topobathymetric lidar data. In Bréhat (turbid) and Saint-Barthélémy (clear), water depth was best modelled using the eight-band dataset with good contributions of yellow and green 1 for Bréhat (R^2=0,77), and purple and green 1 for Saint-Barthélémy (R^2=0,95). The very clear waters of Teti'aroa were best modelled using the combination of base (blue, green 2, red and near-infrared) + yellow (R^2=0,68). The lower accuracy of bathymetry mapping in Teti'aroa revealed biases due to satellite-lidar collection time difference, lidar data specificities, and/or control quality.

1. INTRODUCTION

1.1 Bathymetry Meaningfulness

Oceans and seas are meshed of trade roads, energy pipes and communication cables, that strongly structure today's global human processes. Nevertheless, in 2023, less than 10% of the world's oceans and seas have been mapped using reliable technology, according to the authoritative United States National Oceanic and Atmospheric Administration. This lack of fundamental knowledge might yet considerably exacerbate geopolitical and social-ecological issues in the context of ongoing human pressures and ocean-climate changes.

The coastal fringes of oceans and seas host 40% of the worldwide human population, according to the United Nations, and concentrate one of the highest rates of biodiversity in estuaries, tidal and salt marshes, mangroves, coral reefs, and seagrasses' ecosystems. Those social-ecological systems are increasingly vulnerable to extreme sea levels, predictable by bathymetry-based numerical modelling (Collin et al., 2020).

1.2 Satellite-Derived Bathymetry

Airborne lidar (Collin et al., 2022a) and waterborne sonar (Bulot et al., 2022) surveys of coastal waters are deemed as reference technologies for accurately and precisely bathymetry mapping. However, these techniques are time-consuming and expensive in material and person costs. While the flight missions are restricted to mild and visible air conditions, navigation in shallow coastal waters can be challenging and even dangerous in turbulent waters (Guenther et al., 2000).

The development of spaceborne platforms and sensors, as well as ocean optics have jointly laid the foundation for remotely deriving bathymetry from light backscattering in coastal milieus where both clarity and depth enable it. Satellite-derived bathymetry (SDB) has therefore increased in spatial resolution for the last five decades: from 100 m (Polcyn, 1976) to 0.3 m (Collin et al., 2021a). SDB has also gained in reliability thanks to the refinement in spectral resolution, inherent to the multiplication of spectral bands (Brando et al., 2009). In parallel with hyperspectral-based analytical modelling, the empirical approaches have improved the SDB performances using machine learners, such as linear models (Collin et al., 2017), shallow neural networks (Collin and Hench, 2015), or deep neural networks (Wilson et al., 2020). Despite those significant advances, the mapping of coastal bathymetry in cloudy or tidal areas is still restricted to coarse spatial scenes, such as 30-m Landsat-8 (Pacheco et al., 2015) or 10-m Sentinel-2 (Collin et al., 2016) acquisitions, provided with high temporal resolution (15-day and 10-day, respectively). Finer SDB products leveraging a high or even a very high temporal resolution are expected by policy makers and managers responsible for those cloudy or tidal zones of interest.

1.3 SuperDove-Derived Bathymetry

The very high temporal resolution provided by Planetscope Dove and Dove-R imagery (world's land mass at 3 m pixel size, every day, with four spectral bands, blue, green, red and near-infrared, Table 1) has significantly improved the satellite capabilities to observe the ground or surface water on areas regularly covered by clouds for the last five years (Collin et al.,

* Corresponding author

2022b). Some researchers have tested that 4-band CubeSat constellation to derive the SDB in the coastal areas (Gabr et al., 2020, Li et al., 2019, Poursanidis et al., 2019). The vertical accuracies of the results varied between 0,32 and 1,58 m RMSE (root mean squared error), depending on the age of constellation (Dove or Dove-R) and the methodology used (empirical or semi-empirical modelling).

Since two years, the SuperDove satellites augmented the constellation from a spectral viewpoint. A dataset of eight spectral bands (purple, blue, green 1, green 2, yellow, red, red edge and near-infrared, Table 1) is now acquired with the same spatio-temporal specificities (3-m pixel size and 1-d revisit). A single study has been conducted for river bathymetry mapping using SuperDove (Niroumand-Jadidi et al., 2022). The accuracies of the results ranged between 0,35 and 3,44 RMSE depending on the type of river (Potomac and Colorado) and retrieval algorithm (band ratio and neural network). Regardless of both previous parameters, SuperDove extractions systematically outperformed Dove-R ones.

Band details	Lower band (nm)	Upper band (nm)	Ground Sample Distance (m)
Dove (Classic)			
Blue	455	515	3
Green	500	590	3
Red	590	670	3
Near-infrared	780	860	3
Dove-R			
Blue	464	517	3
Green	547	585	3
Red	650	682	3
Near-infrared	846	888	3
SuperDove			
Purple (Coastal Blue)	431	452	3
Blue	465	515	3
Green 1	513	549	3
Green 2	547	583	3
Yellow	600	620	3
Red	650	682	3
Red Edge	697	713	3
Near-infrared	845	885	3

Table 1. Spectral specifications of the three Planet's sub-constellations (3 × 130 Planetscope CubeSats).

That is why this research will test the contribution of the four novel bands in bathymetry extraction, along a turbidity gradient, using neural networks calibrated, validated, and tested with lidar data. The islands of Bréhat (Channel Sea), Saint-Barthélémy (Caribbean Atlantic Ocean) and Teti'aroa (South Pacific Ocean) are selected to represent that gradient, given the availability of recent topobathymetric lidar data.

2. METHODOLOGY

2.1 Study Islands

Three islands were investigated:

- Bréhat (48°50'N, 03°00'W; 0,2 m^{-1} in 2003-2023 average diffuse attenuation coefficient, KD2) in Brittany (France),
- Saint-Barthélémy (17°54'N, 62°49'W; 0,05 m^{-1} in KD2) in French West Indies, and
- Teti'aroa (17°00'S, 149°33'W; 0,01 m^{-1} in KD2) in French Polynesia (Figure 1).

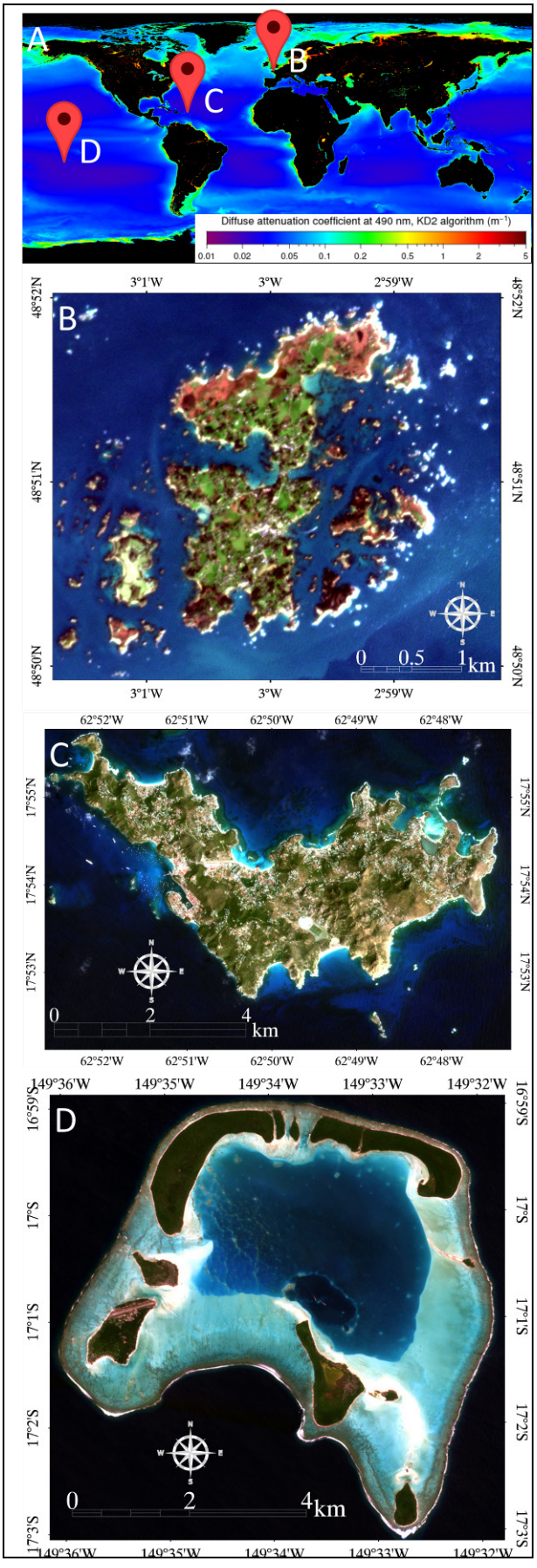

Figure 1. (A) Global 2003-2023 turbidity map with the three islands: (B) Bréhat, (C) Saint-Barthélémy, (D) Teti'aroa.

2.2 SuperDove Imagery

2.2.1 SuperDove Imagery Specifications: The 130 CubeSats (10 cm × 10 cm × 30 cm), related to the 3rd generation of the Planetscopes sun-synchronously orbit at 475 km, collect scenes with ±25° imaging angles, thus covering Earth's land mass from 81,5° South latitude to 81,5° North latitude at 3 m pixel size.

2.2.2 SuperDove Imagery Processings: SuperDove imagery of the three islands were firstly filtered out by incidence angle (<10°), scene percent (100%) and cloud coverage (<1%). Since the acquisition of the imagery usually happens on late morning (local solar time), imageries were collected on:

- 6 March 2021 (11h15 min UTC) for Bréhat,
- 5 March 2021 (14h04 min UTC) for Saint-Barthélémy, and
- 16 October 2022 (19h12min UTC) for Teti'aroa islands.

Bréhat's date corresponds to early spring (temperate northern hemisphere), Saint-Barthélémy's and Teti'aroa's dates fit with dry tropical season.

Imageries were secondly corrected for geometric distortions (orthorectification), and thirdly radiometrically-corrected, from digital numbers to top-of-atmosphere radiance until bottom-of-atmosphere reflectance (unitless).

2.3 Lidar Data

2.3.1 Lidar sources: The three islands were selected according to the availability of recent topobathymetric airborne lidar provided with multiple soundings per m^2. Specifications of the campaigns could be found out at the finest details:

- Bréhat was surveyed in 2021 by French Hydrographic Service, Shom, jointy with IGN and Brittany Region (Shom, 2022, Figure 2A),
- Saint-Barthélémy was monitored in 2018 by Shom jointly with IGN and Saint-Barthélémy's collectivity (Shom-IGN, 2019, Figure 2B) to characterize the impacts of devastating hurricanes (including category 4 Harvey and Jose, and category 5 Irma and Maria),
- Teti'aroa was mapped in 2017 by ETH Zurich (Ural et al., 2019, Figure 2C).

2.3.2 Lidar processings: A procedure of layer stacking enabled to combine eight-band SuperDove corrected imagery with lidar topobathymetric data (0 m as the mean sea level) for every island in order to focus on marine areas. First, the near-infrared reflectance derived from SuperDove imagery was meaningful to distinguish immersed (<0,1 reflectance) from emerged (>0,1 reflectance) areas during the satellite imagery acquisition. Second, the topobathymetry elevation (altitude and depth) was retrieved under the near-infrared sea-land boundary. The sea level elevation was finally validated with the closest tide gauge (Saint-Quay-Portrieux, Deshaies, and Papeete, respectively). The sea level of the SuperDove imagery was thereafter quantified at:

- 3,74 m for Bréhat,
- 0,19 m for Saint-Barthélémy, and
- 0,1 m for Teti'aroa.

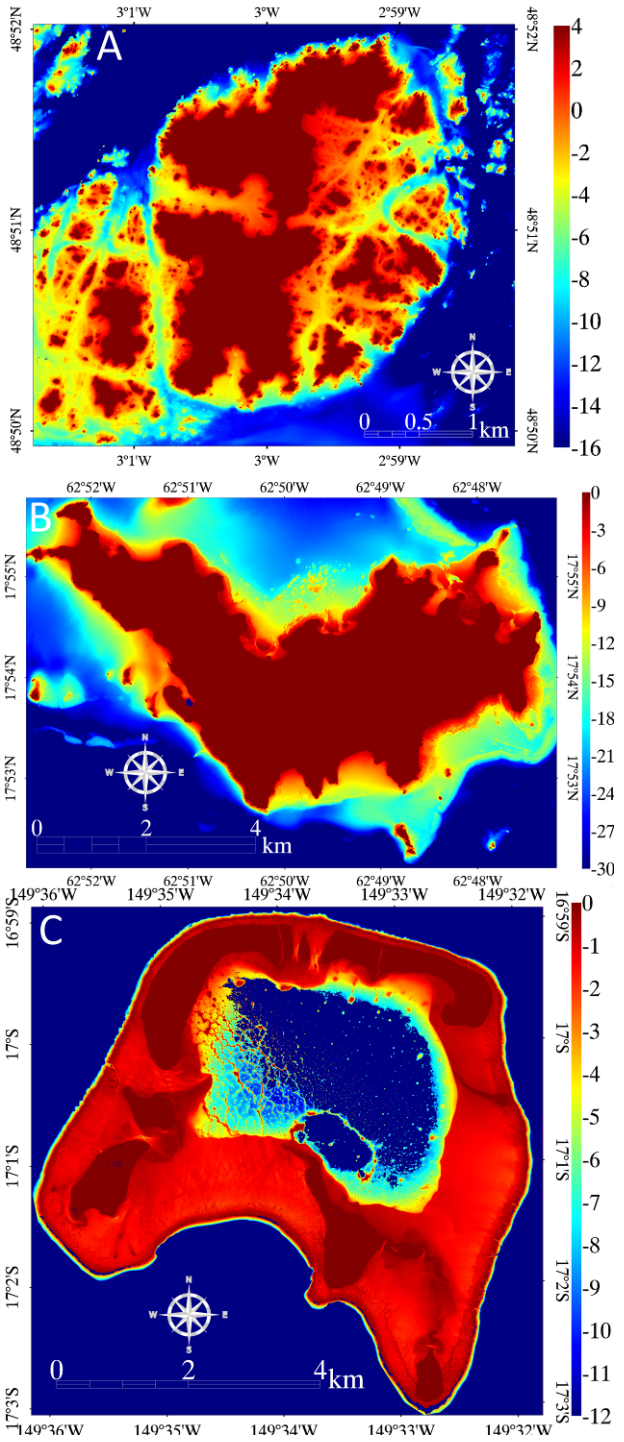

Figure 2. Lidar topobathymetry (0 m as the mean sea level) for (A) Bréhat, (B) Saint-Barthélémy, (C) Teti'aroa islands.

2.4 Neural Network Modelling

Sea level-adjusted lidar measurements were sliced at 0,1 m lag according to associated vertical accuracy statements, resulting in 100, 250 and 120 water classes, for Bréhat, Saint-Barthélémy and Teti'aroa islands, respectively. Density slices were exported as vector files then imported as regions of interests using ENVI software. The regions of interests were screened based on a 90-pixel equalized random sampling in order to balance the calibration of the regression learner, or regressor. Every slice was then split into 30 calibration, 30 validation and 30 test

pixels. For every island, an array of six neural networks were each designed with one layer and three neurons (hyperbolic tangent as activation function, Figure 3):

- blue + green 2 + red + near-infrared, as the base,
- base + purple,
- base + green 1,
- base + yellow,
- base + red edge,
- base + four novel bands.

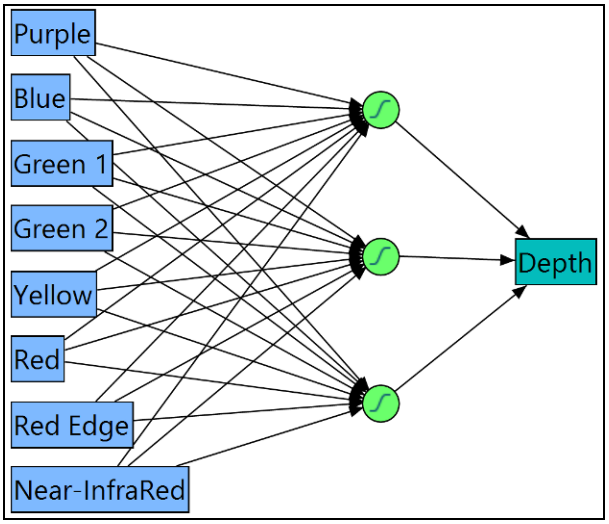

Figure 3. Architecture of the neural network bathymetry model.

3. RESULTS AND DISCUSSION

3.1 Model Accuracy

Bathymetry neural network modelling of Bréhat, Saint-Barthélémy, and Teti'aroa started with R^2_{test} of 0,76, 0,94, and 0,65 for the four-band base datasets, respectively (Figure 4). The best models were achieved with the base + yellow for Tetia'roa (R^2_{test} = 0,68), and with the eight-band datasets for both Saint-Barthélémy and Bréhat (R^2_{test} of 0,95 and 0,77, respectively).

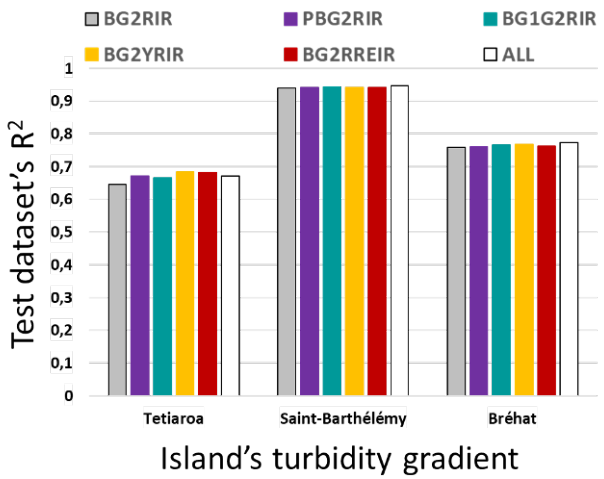

Figure 4. Bathymetry model accuracy based on the SuperDove datasets for the three islands (P: purple, B: blue, G1: green 1, G2: green 2, Y: yellow, R: red, RE: Red edge; IR: near-infrared).

The SuperDove SDB modelling showed significantly better results (μ=0,94±0,002) for Saint-Barthélémy (clear tropical waters) than for Bréhat (μ=0,76±0,005, turbid temperate waters). This comparison indicates that the neural network modelling is better for clearer waters. However, this tendency was not found in Teti'aroa (μ=0,67±0,014), where the water was even clearer than in the lagoon of Saint-Barthélémy (see Figure 1A). This might be explained by three potential factors: water depth, lidar data, and time acquisition. The three islands displayed three distinct maximal depths: 12 m for Teti'aroa, 25 m for Saint-Barthélémy, and 10 m for Bréhat. It will be informational to further examine the results of the models for all 10 m or even from 1 to 10 m gradually. Another explanation may be the differences in lidar acquisition and processing methods amongst the study sites. While Saint-Barthélémy's and Bréhat's zones leveraged the Leica HawkEye-3 sensor (Shom 2019, 2022) providing 1,5 × Secchi Depth, Teti'aroa used the Riegl VQ-820-G system (Ural et al., 2019) providing 1 × Secchi Depth. Even if the point density was greater for Teti'aroa (15 pts.m^{-2}), compared to both other islands (4 pts.m^{-2}), the quality of the cleaning procedure (removal of outliers) might explain the weaker results in Teti'aroa, especially given that the lidar processing was not supervised by an official hydrographic office, like both other islands. Finally, Bréhat and Saint-Barthélémy islands benefited from shorter time differences between lidar and SuperDove data collections (0 and 3 years, respectively) than Teti'aroa one (5 years), likely to bias SBD over mobile sand banks.

3.2 Band-Scale Contribution

In-depth analyses of the SuperDove novel band contribution highlighted greater improvements for Teti'aroa, then Bréhat, and finally Saint-Barthélémy (Figure 5). Yellow, red edge, purple and green 1 decreasingly augmented the base SDB. It might reflect that improved areas were primarily tied to shallower zones, like mobile sand banks. Teti'aroa's eight-band did not produce the best results, perhaps due to confusion generated between conflicting purple-green 1 and yellow-red edge groups.

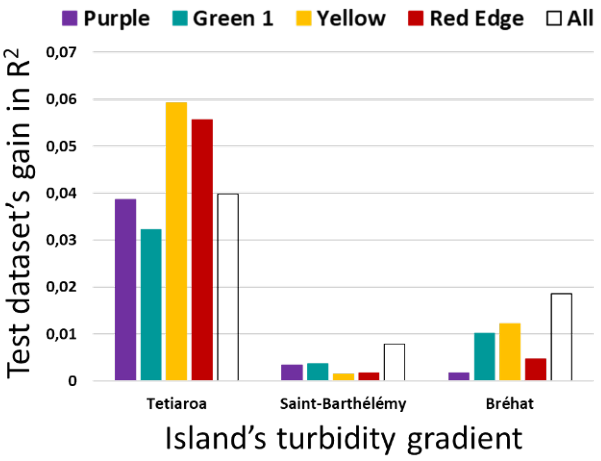

Figure 5. Bathymetry model gain of the SuperDove four novel bands for the three islands.

Regarding Shom's quality level products, the eight-band datasets yielded the best results. Purple and green 1 bands were the best contributors for Saint-Barthélémy (clear waters) and yellow and green 1 bands enhanced Bréhat (turbid waters). The first outcome corroborates the great interest of the so-called

"coastal" band to refine bathymetry with more energetic wavelengths when water clarity enables it. The second outcome underlines the importance to get information in yellow waveband to estimate colored dissolved organic matter in unclear coastal waters (Collin and Planes, 2011).

3.3 Best Model For Bathymetry Mapping

Bréhat and Saint-Barthélémy's best models were based on the eight-band neural networks (Figure 6A and 6B, respectively), while the base + yellow was selected for Teti'aroa (Figure 6C). Their respective vertical accuracies were 1,19; 1,57 and 1,58 m.

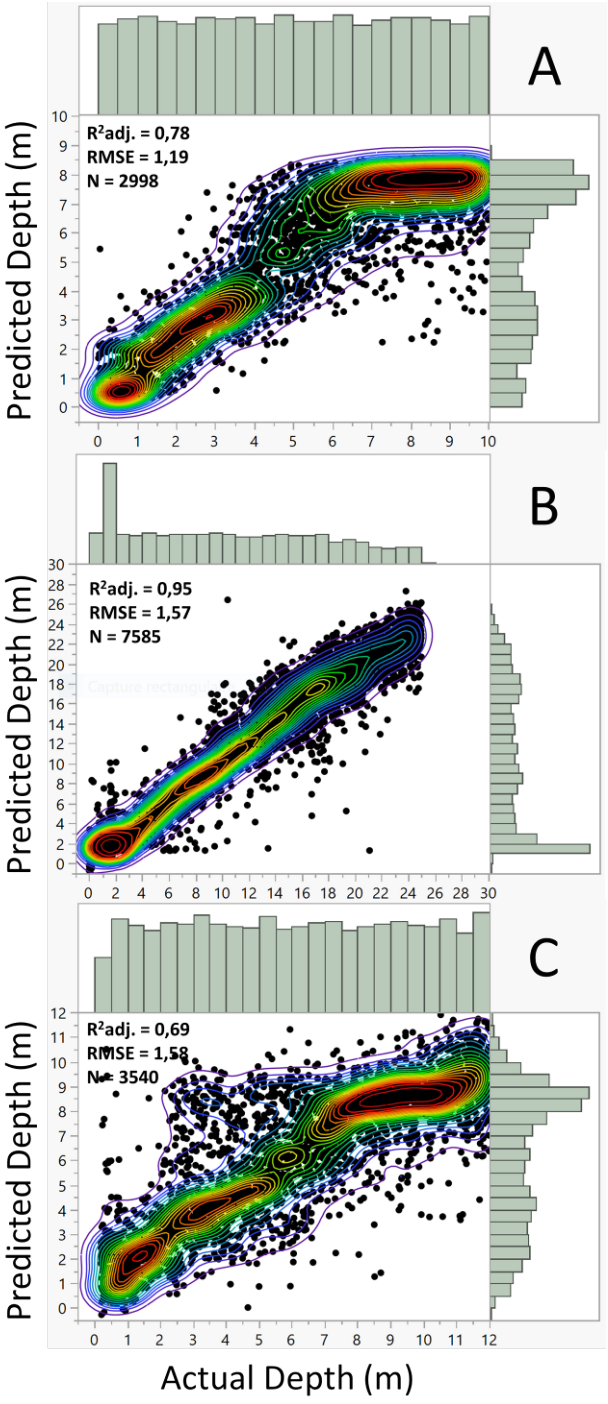

Figure 6. Best bathymetric neural network predictions for (A) Bréhat, (B) Saint-Barthélémy, (C) Teti'aroa islands.

The three best formulae, derived from the models, allowed each to rasterize the three neurons to finally map the water depth for Bréhat, Saint-Barthélémy, and Teti'aroa (Figure 7A, 7B, and 7C). The well predicted maximum depth revolves around 8 m for both Bréhat and Teti'aroa, and 25 m for Saint-Barthélémy. Deeper investigations over the waters of this island might reach 30-m estimates of the WorldView-2 in Moorea (Collin and Hench, 2012). The development of richer (neurons) and/or deeper (layers) neural networks, such as convolutional ones (Collin et al., 2021b), holds great promise.

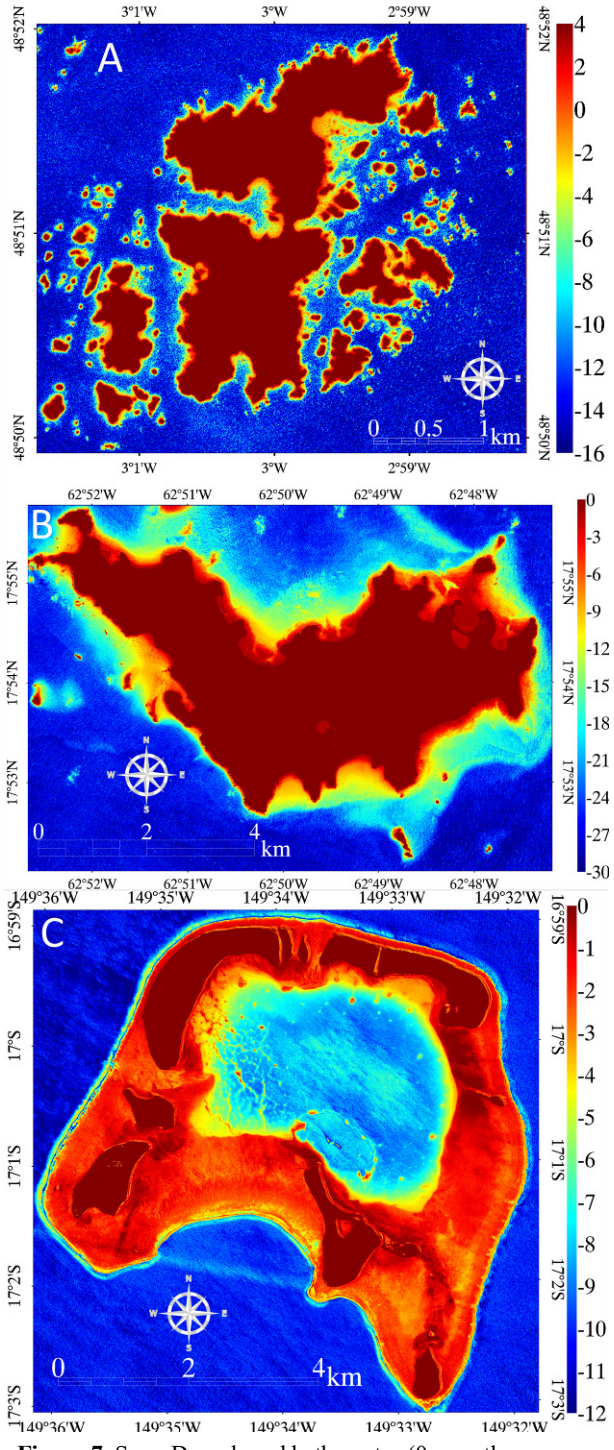

Figure 7. SuperDove-based bathymetry (0 m as the mean sea level) for (A) Bréhat, (B) Saint-Barthélémy, (C) Teti'aroa islands.

4. CONCLUSIONS

SuperDove-based bathymetry was modelled over three island waters (from 0,01 to 0,2 m^{-1} in KD2) using one-layered three-neuroned models calibrated / validated / tested with lidar data. Bréhat turbid and Saint-Barthélémy clear water depths were best modelled using the eight-band dataset with good contributions of yellow and green 1 for Bréhat (R^2=0,77), and purple and green 1 for Saint-Barthélémy (R^2=0,95). The very clear waters of Teti'aroa were best modelled using the base + yellow combination (R^2=0,68), revealing biases due to satellite-lidar collection time difference, lidar data specificities, and/or control quality.

REFERENCES

Brando, V.E., Anstee, J.M., Wettle, M., Dekker, A. G., Phinn, S.R., Roelfsema, C., 2009: A physics based retrieval and quality assessment of bathymetry from suboptimal hyperspectral data. *Remote sensing of Environment*, 113(4), 755-770.

Bulot, A., Collin, A., Letard, M., Feunteun, E., Le Goff, L., Pastol, Y., Caline, B., 2022: Spatial Modeling of the Benthic Biodiversity Using Topo-Bathymetric Lidar and Neural Networks. *European Spatial Data for Coastal and Marine Remote Sensing: Proceedings of International Conference EUCOMARE 2022-Saint Malo*, France, 223-227.

Collin, A., Andel, M., Lecchini, D., Claudet, J., 2021a: Mapping Sub-Metre 3D Land-Sea Coral Reefscapes Using Superspectral WorldView-3 Satellite Stereoimagery. *Oceans*, 2(2), 315-329.

Collin, A., Calle, C., James, D., Costa, S., Maquaire, O., Davidson, R., Trigo-Teixeira, A., 2020: Modelling 2D coastal flooding at fine-scale over vulnerable lowlands using satellite-derived topobathymetry, hydrodynamic and overflow simulations. *Journal of Coastal Research*, 95(SI), 1052-1056.

Collin, A., Etienne, S., Feunteun, E., 2017: VHR coastal bathymetry using WorldView-3: colour versus learner. *Remote Sensing Letters*, 8(11), 1072-1081.

Collin, A., Hench, J.L., 2015: Extracting shallow bathymetry from very high resolution satellite spectral bands and a machine learning algorithm. *International Council of the Exploration of the Sea,* CM, 24.

Collin, A., Hench, J.L., 2012: Towards deeper measurements of tropical reefscape structure using the WorldView-2 spaceborne sensor. *Remote Sensing*, 4(5), 1425-1447.

Collin, A., James, D., Feunteun, E., 2022b: Towards better coastal mapping using fusion of high temporal Sentinel-2 and PlanetScope-2 imageries: 12 bands at 3 m through neural network modelling. *The Inter. Arch. Photo., Rem. Sens. and Spa. Inf. Sci.*, 43, 479-484.

Collin, A., Laporte, J., Koetz, B., Martin-Lauzer, F.R., Desnos, Y.L., 2016: Mapping bathymetry, habitat, and potential bleaching of coral reefs using Sentinel-2. *13th International Coral Reef Symposium*, 405-420.

Collin, A., Letard, M., Andel, M., Sharma, S., 2021b: Object-based mangrove mapping using submeter superspectral WorldView-3 imagery and deep convolutional neural network. *IEEE IGARSS*, 7362-7365.

Collin, A., Pastol, Y., Letard, M., Le Goff, L., Guillaudeau, J., James, D., Feunteun, E., 2022a: Increasing the Nature-Based Coastal Protection Using Bathymetric Lidar, Terrain Classification, Network Modelling: Reefs of Saint-Malo's Lagoon?. *European Spatial Data for Coastal and Marine Remote Sensing: Proceedings of International Conference EUCOMARE 2022-Saint Malo*, France, 235-241.

Collin, A., Planes, S., 2011: What is the value added of 4 bands within the submetric remote sensing of tropical coastscape? Quickbird-2 vs WorldView-2. *IEEE IGARSS*, 2165-2168).

Gabr, B., Ahmed, M., Marmoush, Y., 2020: PlanetScope and landsat 8 imageries for bathymetry mapping. *Journal of Marine Science and Engineering*, 8(2), 143.

Guenther, G.C., Cunningham, A.G., LaRocque, P.E., Reid, D.J., 2000: Meeting the accuracy challenge in airborne lidar bathymetry. *Proceedings of EARSeL-SIG-Workshop LIDAR*. pp. 1–28.

Li, J., Knapp, D. E., Schill, S. R., Roelfsema, C., Phinn, S., Silman, M., ..., Asner, G. P., 2019: Adaptive bathymetry estimation for shallow coastal waters using Planet Dove satellites. *Remote Sensing of Environment*, 232, 111302.

Niroumand-Jadidi, M., Legleiter, C. J., Bovolo, F., 2022 : River Bathymetry Retrieval From Landsat-9 Images Based on Neural Networks and Comparison to SuperDove and Sentinel-2. *IEEE J-STARS*, 15, 5250-5260.

Pacheco, A., Horta, J., Loureiro, C., Ferreira, Ó., 2015: Retrieval of nearshore bathymetry from Landsat 8 images: A tool for coastal monitoring in shallow waters. *Remote Sensing of Environment*, 159, 102-116.

Polcyn, F.C., 1976: NASA/Cousteau ocean bathymetry experiment. Remote bathymetry using high gain LANDSAT data (No. ERIM-118500-1-F).

Poursanidis, D., Traganos, D., Chrysoulakis, N., Reinartz, P., 2019 : Cubesats allow high spatiotemporal estimates of satellite-derived bathymetry. *Remote Sensing*, 11(11), 1299.

Shom - IGN, 2022.
https://doi.org/10.17183/L3D_MAR_BZH_2018_2021

Shom-IGN, 2019.
http://dx.doi.org/10.17183/L3D_SAINT_BARTHELEMY_2019

Tonion, F., Pirotti, F., Faina, G., Paltrinieri, D., 2020 : A machine learning approach to multispectral satellite derived bathymetry. *ISPRS Annals of the Photogrammetry, Remote Sensing and Spatial Information Sciences*, 3, 565-570.

Ural, S., Gruen, A., Kocaman, S., 2019: Point clouds over Tetiaroa - 3D modeling of a tropical island by topo-bathymetric lidar. *Proceedings of the Asian Conference of Remote Sensing*, Daejeon, Korea, 13–19 October.

Wilson, B., Kurian, N. C., Singh, A., Sethi, A., 2020: Satellite-derived bathymetry using deep convolutional neural network. *IEEE IGARSS*, 2280-2283.